atmosphere

MDPI

Article

Deciphering Reservoir Storage Variability: A Multi-Reservoir Assessment of Hydroclimatic Drought Responses in Northwestern Türkiye

Fatma Yaman Öz [1,*], Esra Eren [2], Emre Özelkan [3,4], Hasan Tatli [5] and Muhittin Karaman [6]

[1] Department of Geography, School of Graduate Studies, Çanakkale Onsekiz Mart University, 17020 Çanakkale, Türkiye
[2] Department of Landscape Architecture, Graduate School of Education, Çanakkale Onsekiz Mart University, 17020 Çanakkale, Türkiye; esraa.eeren@gmail.com
[3] Department of Urban and Regional Planning, Faculty of Architecture and Design, Çanakkale Onsekiz Mart University, 17020 Çanakkale, Türkiye; emreozelkan@comu.edu.tr
[4] Department of Natural Disaster Risk Management, School of Graduate Studies, Çanakkale Onsekiz Mart University, 17020 Çanakkale, Türkiye
[5] Climatology/Meteorology, Physical Geography Division, Department of Geography, Faculty of Humanities and Social Sciences, Çanakkale Onsekiz Mart University, 17020 Çanakkale, Türkiye; tatli@comu.edu.tr
[6] Department of Geological Engineering, Faculty of Mines, Istanbul Technical University, 34469 Istanbul, Türkiye; mkaraman@itu.edu.tr
* Correspondence: fatmayamanoz.comu@gmail.com

Abstract

Climate change, rising water demand, and land use change are increasing the complexity of reservoir management. This study evaluates reservoir storage responses to hydroclimatic drought across 12 reservoirs in the Marmara, Susurluk, Meriç–Ergene, and Northern Aegean basins of northwestern Türkiye. Data from 27 meteorological stations were used to calculate the SPI, SPEI, and RDI at 1-, 3-, 6-, 9-, and 12-month scales. Reservoir storage during 2013–2022 was evaluated seasonally using Random Forest (RF), Linear Models (LMs), and Generalized Additive Models (GAMs) under leave-one-year-out cross-validation (LOYO-CV). The agricultural-area NDVI and reservoir characteristics provided contextual information rather than direct measures of water withdrawal. Drought indices at 6–12-month scales were selected as dominant predictors for 11 of the 12 reservoirs. RF was the best performing model in 20 of 48 reservoir–season combinations, compared with 16 for LMs and 12 for GAMs, although performance varied among reservoirs and seasons. Basin mean and reservoir local drought series were strongly correlated (mean $r = 0.88$), whereas Local-IDW representation did not systematically improve performance. Nevertheless, dominant predictors changed in eight reservoirs, highlighting local hydroclimatic heterogeneity. The agricultural NDVI showed considerable temporal and spatial variability but was not interpreted as evidence of reservoir-specific withdrawals or anthropogenic causation. Overall, reservoir drought sensitivity reflects cumulative hydroclimatic conditions and pronounced seasonal and reservoir-specific variability. The integrated cross-validation and spatial sensitivity framework provides a rigorous basis for reservoir drought assessment and adaptive water resource management.

Keywords: reservoir storage; hydroclimatic drought; drought indices; NDVI; cross-validation; water resource management

Check for updates

Academic Editors: Emma Gaitán Fernández and María Rosa Pino-Otín

Received: 3 August 2026
Revised: 17 September 2026
Accepted: 17 September 2026
Published: 21 September 2026

Copyright: © 2026 by the authors. Licensee MDPI, Basel, Switzerland. This article is an open access article distributed under the terms and conditions of the Creative Commons Attribution (CC BY) license.

1. Introduction

Freshwater resources are fundamental to ecosystems, agriculture, and human well-being [1]. However, climate change, population growth, and urbanization increasingly challenge sustainable water management [2,3]. In this context, dams regulate streamflow and secure water supply during droughts [4], making reservoir storage dynamics key indicators of reliability and resilience under changing hydroclimatic conditions [5].

Dams provide multiple services, including irrigation, drinking water supply, hydropower, flood control, and ecosystem support [6], and are increasingly recognized as important components of climate adaptation and water security [7]. However, increasing drought frequency and severity can threaten reservoir reliability [2,5,8], as reduced precipitation and increased evaporative demand may decrease inflows and water availability [9,10]. Understanding reservoir responses to drought is therefore important for effective water resource management [11].

Drought is a slow-onset phenomenon whose effects may persist for months or years [8,12,13]. Declining precipitation and increasing evapotranspiration can reduce runoff and reservoir inflows [14,15]. However, reservoirs exposed to similar climatic conditions may respond differently depending on catchment characteristics, storage capacity, antecedent hydroclimatic conditions, and water demand [16,17]. Identifying the temporal and spatial characteristics of these drought–storage relationships is therefore important for adaptation and reservoir management [18].

Widely used drought indicators include the Standardized Precipitation Index (SPI), Standardized Precipitation–Evapotranspiration Index (SPEI), and Reconnaissance Drought Index (RDI) [19,20]. Unlike the SPI, which is based solely on precipitation, the SPEI and RDI incorporate potential evapotranspiration and therefore account for atmospheric water demand [9,21]. Short accumulation scales primarily characterize short-term meteorological anomalies, whereas longer scales reflect cumulative water deficits that may influence soil moisture, runoff, recharge, and reservoir storage [22–25]. Evaluating multiple indices and accumulation periods is important because drought–storage relationships may vary among reservoirs and seasons.

Reservoir storage may also be influenced by human activities, including irrigation withdrawals, land use change, and other forms of water demand [8,14,26–28]. Direct separation of climatic and anthropogenic contributions, however, requires reservoir-specific information on withdrawals, inflows, releases, and operating rules, which is often unavailable over sufficiently long and consistent periods. Where such data are unavailable, land use characteristics, reservoir functions, irrigated areas, crop patterns, and vegetation dynamics can provide contextual information, but should not be interpreted as direct quantitative measures of human water use. Remote sensing observations of Acıgöl in western Türkiye similarly revealed pronounced temporal variations in water-covered area, illustrating the sensitivity of inland water bodies to climatic variability and concurrent human water use [28].

Mediterranean-scale studies indicate that climate change, increasing water demand, and prolonged drought may reduce reservoir inflows, decrease water availability, and increase uncertainty in water resource management [29,30]. According to Gorguner and Kavvas [31], Berhail and Katipoğlu [32], and Montaldo et al. [33], Türkiye is particularly vulnerable to these changes, with evidence of increasingly dry conditions and greater drought severity affecting water resources and other climate-sensitive sectors [34].

Previous studies in the Marmara and Northern Aegean regions have examined drought, reservoir dynamics, and water management from different perspectives. Studies of Atikhisar Dam indicated that meteorological drought alone may not fully explain reservoir variability [35,36], while remote sensing studies have documented reservoir changes

during severe drought periods [37,38]. Other studies have highlighted the relevance of irrigation demand, changing inflows, ecosystem sensitivity, and reservoir management in the region [39–41]. At the reservoir scale, Karaman and Özelkan [42] demonstrated for Bayramiç Dam Lake that hydro-meteorological factors primarily influence water inputs, whereas anthropogenic factors, particularly irrigation and hydropower-related water use, can substantially affect reservoir outputs. Nevertheless, an important question remains insufficiently addressed: how robust are reservoir-specific drought–storage relationships when they are evaluated across different seasons, modeling approaches, drought timescales, and spatial representations of drought? Addressing this question is particularly important in hydroclimatically heterogeneous regions where basin-averaged conditions may not fully represent the drought signal experienced by individual reservoirs.

Machine learning and advanced statistical methods provide complementary approaches for examining these relationships [43,44]. Random Forest (RF) can represent complex interactions among predictors, Generalized Additive Models (GAMs) can characterize potentially nonlinear relationships, and Linear Models (LMs) provide a comparatively simple statistical benchmark [5,11,17]. However, comparison of these approaches requires a common out-of-sample validation framework, particularly when relatively short hydrological records, correlated drought indicators and alternative drought representations are involved. Moreover, the robustness of reservoir-specific drought predictors to the spatial representation of drought remains important when substantial within-basin hydroclimatic heterogeneity exists.

Accordingly, the primary objective of this study is to evaluate the temporal and spatial robustness of reservoir storage responses to hydroclimatic drought across twelve reservoirs in four basins of northwestern Türkiye. Specifically, this study aims to (i) characterize drought conditions using the SPI, SPEI, and RDI at multiple accumulation timescales; (ii) quantify seasonal drought–storage relationships using RF, GAMs, and LMs under a common leave-one-year-out cross-validation (LOYO-CV) framework; (iii) distinguish predictive performance from exploratory statistical evidence; and (iv) assess the sensitivity of reservoir-specific results to drought representation by comparing basin mean indices with reservoir local, distance-weighted indices. Reservoir function, irrigated area, crop characteristics, and the growing season NDVI derived exclusively from CORINE agricultural land cover classes are additionally considered contextual information on potential anthropogenic influences rather than as direct quantitative measures of water withdrawals.

The methodological contribution of this study lies not in the individual application of established drought indices or modeling techniques, but in their integration within a common validation and spatial sensitivity framework. By comparing RF, GAMs, and LMs under identical temporal validation procedures and evaluating the sensitivity of dominant predictors to alternative drought representation, this study provides a more rigorous basis for identifying reservoir-specific drought sensitivity. Its application across twelve reservoirs with contrasting hydroclimatic settings enables regionally consistent drought signals to be distinguished from reservoir-specific responses. Because reservoir command-area boundaries, direct irrigation withdrawals, and consistent municipal demand records were unavailable, this study does not attempt to provide causal attribution of storage changes to human water use.

2. Materials and Methods

This study evaluates reservoir storage responses to hydroclimatic drought across twelve reservoirs in northwestern Türkiye. The analysis comprises four main stages: (i) data preparation and drought characterization; (ii) seasonal reservoir drought modeling

and out-of-sample validation; (iii) statistical inference and spatial sensitivity assessment; and (iv) contextual evaluation of agricultural and reservoir characteristics.

2.1. Study Area

This study covers the Marmara, Northern Aegean, Susurluk, and Meriç–Ergene basins in northwestern Türkiye (Figure 1). Based on the Aridity Index (AI = P/PET), Marmara, Northern Aegean, and Meriç–Ergene are semi-arid, whereas Susurluk is arid. The reservoirs provide drinking water (Doğancı, Ömerli, Terkos, and Yuvacık), irrigation (Altınyazı, Bakacak, and Karaidemir), combined irrigation and drinking water supply (İkizcetepeler, Ayvacık, Atikhisar, and Kırklareli), or irrigation and hydropower (Bayramiç). Water-demanding crops, including rice and maize, are cultivated in agricultural areas associated with several irrigation reservoirs and provide context for seasonal water demand.

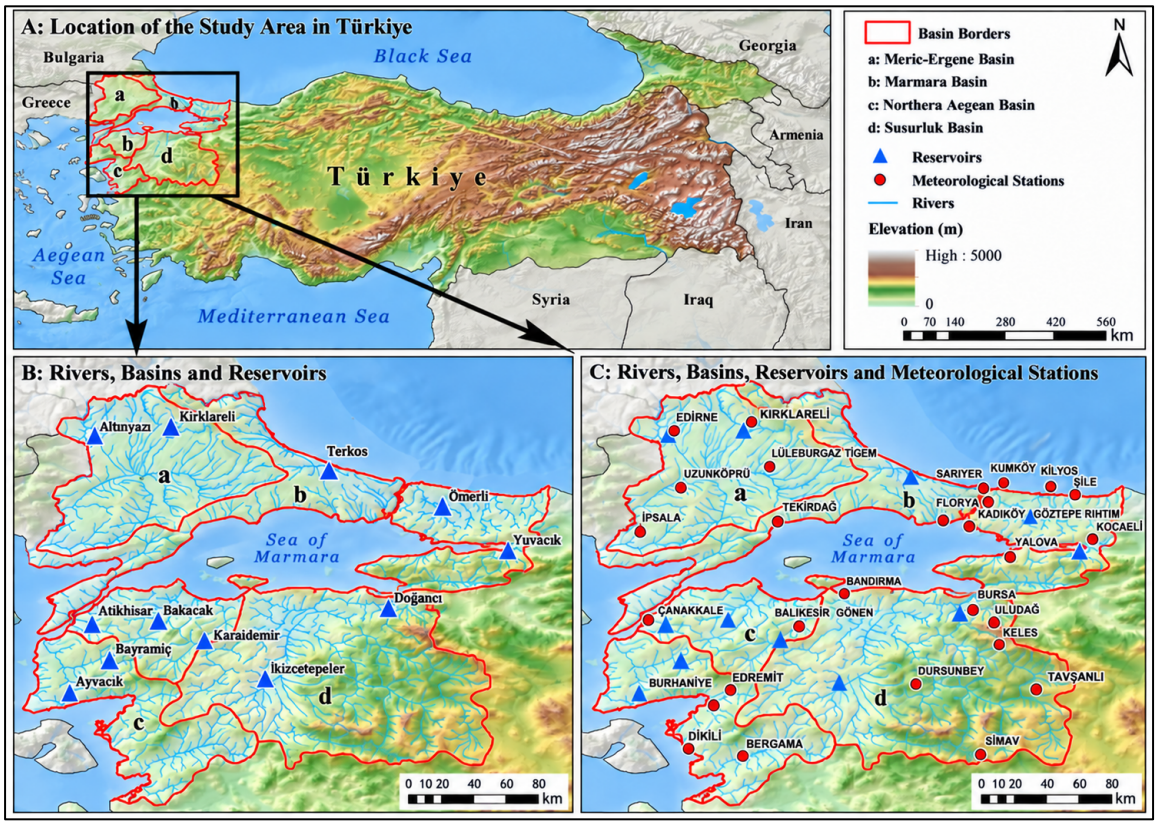


Figure 1. The study area and spatial distribution of the hydrological basins, reservoirs, river network and meteorological stations used for drought and reservoir analyses in northwestern Türkiye. (**A**) The location of the study area within Türkiye. (**B**) Basin boundaries, rivers and reservoirs. (**C**) The distribution of meteorological stations together with basin boundaries, rivers and reservoirs.

The Marmara Basin has transitional characteristics between Mediterranean summer aridity and year-round Black Sea rainfall, with annual precipitation of 682 mm and a mean temperature of 14.6 °C [45]. It includes Atikhisar, Bakacak, Karaidemir, Ömerli, Terkos, and Yuvacık reservoirs. The Northern Aegean Basin has a Mediterranean climate characterized by summer drought and high evaporative demand (652 mm; 16.5 °C) and is represented by Ayvacık and Bayramiç reservoirs [46]. The Susurluk Basin, represented by Doğancı and İkizcetepeler, receives maritime influence but experiences summer drought (731 mm; 12.7 °C) [47]. The Meriç–Ergene Basin combines Black Sea, Marmara, and continental influences, contains extensive agricultural plains, and is represented by Altınyazı and Kırklareli reservoirs (602 mm; 13.8 °C) [46].

Topographic contrasts in Marmara and the Northern Aegean and extensive plains in Susurluk and Meriç–Ergene influence precipitation, runoff, and reservoir recharge. The selected reservoirs therefore provide contrasting hydroclimatic and operational settings for evaluating reservoir-specific drought–storage relationships.

2.2. Data and Analytical Framework

Monthly reservoir storage was evaluated using the SPI, SPEI, and RDI at 1-, 3-, 6-, 9-, and 12-month scales for 2013–2022. Because storage observations represent conditions at the beginning of each month, each value was aligned with drought indices from the preceding month. This represented fixed temporal alignment rather than an optimized reservoir-specific lag. Continuous predictors were standardized within each training fold.

Seasonal responses were assessed using Random Forest (RF), Linear Models (LMs), and Generalized Additive Models (GAMs). After removing missing values, reservoir–season datasets contained 23–29 monthly observations. All models were evaluated using leave-one-year-out cross-validation (LOYO-CV), with predictor screening performed within each training fold. Predictors required an absolute correlation of at least 0.20 with storage; predictors with pairwise correlations of 0.90 or greater were not retained together, and each model included a maximum of three predictors. Performance was assessed using cross-validated R^2, RMSE, and MAE. Post-selection LM inference was evaluated using Benjamini–Hochberg false discovery rate correction, whereas GAMs and RF were used primarily for prediction. All statistical analyses and predictive modelling were performed using R (version 4.4.2; R Core Team, Vienna, Austria) within RStudio (version 2026.04.0+526; Posit Software, PBC, Boston, MA, USA).

The growing season NDVI was calculated for April–September using CORINE 2018 agricultural classes within codes 211–244, with forests and other non-agricultural classes masked as NoData. Because reservoir command-area boundaries and withdrawal records were unavailable, the NDVI, reservoir purpose, irrigated area, and crop characteristics were interpreted as contextual information rather than direct measures of reservoir-specific water withdrawals. Consistent reservoir-specific population and municipal demand data were also unavailable and were not included as quantitative predictors.

The primary analysis used basin mean drought indices. Spatial sensitivity was assessed using Local-IDW series derived from the three nearest stations within each basin through inverse-distance-squared weighting. Both representations were evaluated using identical screening and LOYO-CV procedures. Spatial analyses and map production were performed using ArcMap (version 10.7; Esri, Redlands, CA, USA). The methodological framework is presented in Figure 2.

2.3. Analytical Methods

2.3.1. Drought Indices

Meteorological drought conditions were assessed using three commonly used drought indices: the Standardized Precipitation Index (SPI), the Standardized Precipitation–Evapotranspiration Index (SPEI) and the Reconnaissance Drought Index (RDI). In order to determine the short-, medium- and long-term effects of drought, all indices were calculated on 1-, 3-, 6-, 9- and 12-month time scales.

Standardized Precipitation Index (SPI)

The SPI was calculated following the method developed by McKee et al. [48]. Monthly precipitation totals were evaluated for different accumulation periods, fitted to a gamma probability distribution, and transformed into a standard normal distribution. This method enables the comparison of drought severity across different regions and time

periods [48,49]. Negative SPI values indicate dry conditions, whilst positive values indicate wet conditions (Table 1).

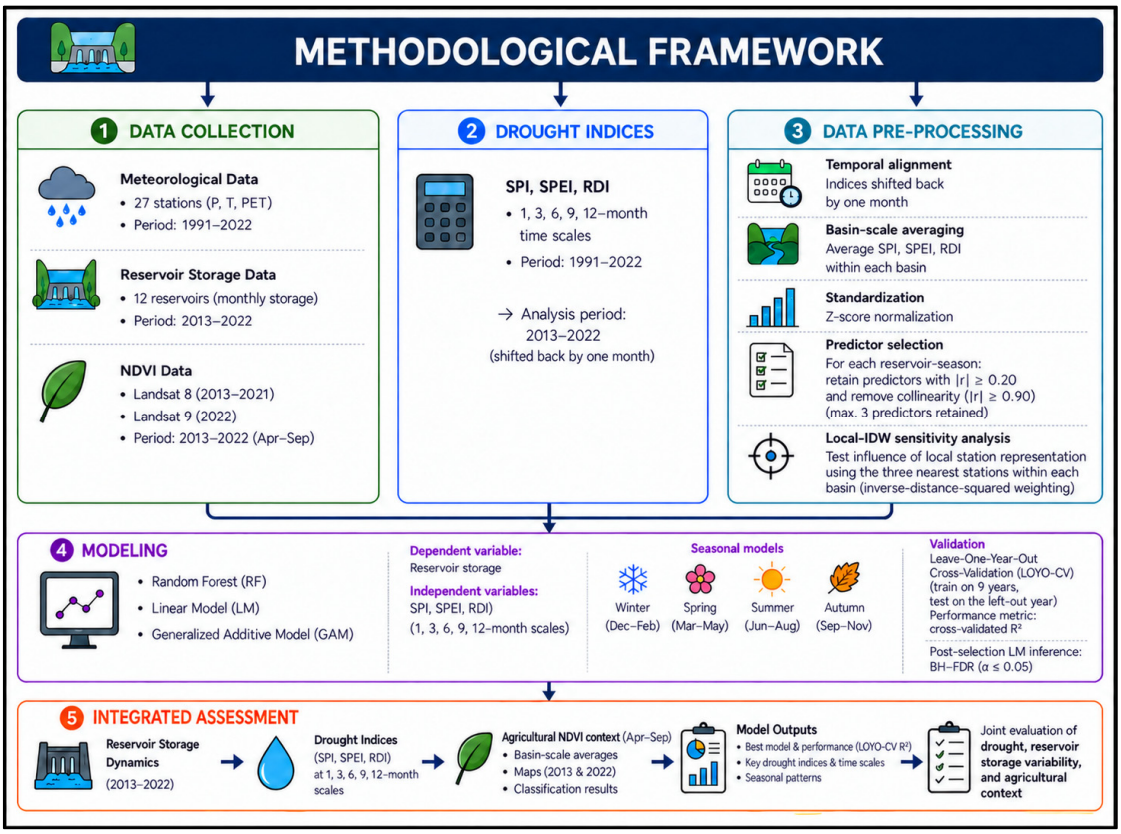


Figure 2. Methodological framework for reservoir storage analysis using drought indices and contextual agricultural NDVI information.

Table 1. Classification of drought and wetness categories based on SPI, SPEI and RDI values.

SPI, SPEI and RDI	Moisture Categories
≥2.0	Extremely Wet
1.5 to 1.99	Severely Wet
1.0 to 1.49	Moderately Wet
0.99 to −0.99	Near Normal
−1.00 to −1.49	Moderate Drought
−1.50 to −1.99	Severe Drought
≤−2.00	Extreme Drought

Standardized Precipitation–Evapotranspiration Index (SPEI)

The SPEI was calculated from the climatic water balance between precipitation and potential evapotranspiration (PET). Monthly PET was estimated from air temperature data using the Hargreaves method, and the climatic water balance was calculated as follows (1):

$$D_i = P_i - PET_i \quad (1)$$

Here, (P_i) represents the monthly precipitation amount, whilst (PET_i) represents the monthly potential evapotranspiration. The resulting water balance series were aggregated across different time scales, fitted to appropriate probability distributions, and standardized to calculate SPEI values [9,50,51]. As it takes into account not only precipitation deficits but

also temperature-driven atmospheric water demand, the SPEI is widely used for assessing drought under climate change conditions.

Reconnaissance Drought Index (RDI)

The RDI was calculated in accordance with the method proposed by Tsakiris et al. [52]. The initial value of the index is defined as follows (2):

$$a_0^{(i)} = \frac{\sum_{j=1}^{12} P_{ij}}{\sum_{j=1}^{12} PET_{ij}} \quad (2)$$

Here, (P_{ij}) and (PET_{ij}) represent the precipitation and potential evapotranspiration values for month (j) in year (i), respectively. The same monthly PET series estimated using the Hargreaves method were used in the RDI calculations. The calculated values were normalized and standardized to make them comparable across different climatic regions and periods [10,52]. As with the SPI and SPEI, negative RDI values indicate dry conditions, whilst positive values indicate wet conditions (Table 1).

All indices were calculated in R, and drought severity was interpreted using the standard classes presented in Table 1 [10].

2.3.2. Statistical and Machine Learning Models

Linear Models (LMs), Generalized Additive Models (GAMs), and Random Forest (RF) were used to evaluate reservoir storage responses to hydroclimatic drought. Separating climatic forcing from other controls is an important issue in water resource research [53]. The selected models represent linear, nonlinear, and machine learning approaches, respectively, allowing their predictive performance to be compared under a common framework [54].

The LM was used as an interpretable baseline for estimating linear relationships between reservoir storage and the selected drought predictors. Its general form is as follows (3) [55]:

$$y = \beta_0 + \sum_{j=1}^{p} \beta_j x_j + \varepsilon \quad (3)$$

where y represents the dependent variable (reservoir storage volume), β_0 is the intercept, β_j is the regression coefficient for the p explanatory variables (x_j), and ε is the random error term.

GAMs were used to represent potentially nonlinear or threshold-type drought–storage relationships through smooth predictor functions. The general structure of a GAM is expressed as follows (4):

$$g[E(Y)] = \beta_0 + \sum_{j=1}^{p} s_j(x_j) \quad (4)$$

where g is the link function relating the expected value of the response variable to the predictors, and $s_j(x_j)$ represents the smooth function applied to the j-th explanatory variable. For the present analysis, GAMs were fitted using restricted maximum likelihood (REML), with the basis dimension restricted to $k = 3$ and shrinkage selection applied to limit model complexity. The low basis dimension was deliberately selected to reduce the risk of overfitting given the small reservoir–season sample sizes (23–29 observations) and the use of out-of-sample LOYO-CV.

RF was used to capture complex relationships and interactions among predictors. It combines regression trees generated through bootstrap sampling and random predictor selection, with the final estimate obtained by averaging their predictions [56]. The RF regression prediction for an input vector x can be expressed as follows (5):

$$\hat{f}(x) = \frac{1}{B} \sum_{b=1}^{B} T_b(x) \quad (5)$$

where B represents the total number of trees and $T_b(x)$ is the prediction generated by the b-th regression tree. In this study, RF models were fitted using 500 trees.

As detailed in Section 2.2, all three models were evaluated using identical LOYO-CV folds and fold-specific predictor screening and standardization. Predictive performance was assessed using out-of-fold R^2, RMSE, and MAE. Negative R^2 values were retained as performance below the mean observation benchmark. Statistical inference was limited to 143 post-selection LM terms and adjusted using the Benjamini–Hochberg false discovery rate procedure $pFDR < 0.05$. Because inference followed predictor selection, these results were considered exploratory; GAMs and RF were evaluated primarily through out-of-sample predictive performance.

2.3.3. Normalized Difference Vegetation Index (NDVI)

The Normalized Difference Vegetation Index (NDVI) is a remote sensing indicator of vegetation greenness and photosynthetic activity based on the contrast between chlorophyll absorption in the red band and vegetation reflectance in the near-infrared (NIR) band [57]. It was calculated as follows (6) [58]:

$$NDVI = \frac{NIR - Red}{NIR + Red} \quad (6)$$

Here, NIR represents the near-infrared band and Red represents the red band of the satellite images.

The NDVI was calculated from Landsat Collection 2 Level-2 Surface Reflectance imagery processed in Google Earth Engine (GEE; Google LLC, Mountain View, CA, USA). Landsat 8 imagery was used for 2013–2021 and Landsat 9 for 2022, with bands 5 and 4 representing NIR and red reflectance, respectively. Annual mean composites were produced for the April–September growing season to represent agricultural vegetation activity during peak crop development.

To minimize the influence of natural vegetation, the CORINE 2018 land cover dataset was integrated into the analysis. Only agricultural classes within codes 211–244 were retained; forests, grasslands, wetlands, settlements, and other non-agricultural classes were masked as NoData. The annual basin-level NDVI was then calculated from the remaining agricultural pixels.

The NDVI theoretically ranges from −1 to +1, and established thresholds provide a general interpretation of vegetation conditions (Table 2) [59–61]. Agricultural thresholds can additionally characterize differences in crop greenness and vegetation condition [62,63]. However, the NDVI measures vegetation greenness rather than irrigation water use. Because reservoir command-area boundaries and reservoir-specific withdrawal records were unavailable, the agricultural NDVI was interpreted as complementary basin-scale information and not as a direct measure of reservoir withdrawals or anthropogenic causation.

2.4. Data Pre-Processing

Reservoir storage observations recorded at the beginning of month (t) were matched with drought indices from the preceding month ($t - 1$). This fixed shift ensured temporal consistency and was not treated as an optimized reservoir-specific hydrological lag. Basin mean drought indices were used in the primary analysis, and continuous predictors were standardized using parameters calculated within each LOYO-CV training fold. Seasonal datasets were prepared for winter (December–February), spring (March–May), summer (June–August), and autumn (September–November).

Reservoir function, irrigated area, crop characteristics, and the agricultural-area NDVI were used only for contextual interpretation. Because reservoir command-area boundaries,

withdrawal records, and consistent reservoir-specific population and municipal demand data were unavailable, these variables were not interpreted as direct quantitative measures of water use or anthropogenic causation.

Table 2. General interpretation of growing season NDVI ranges within CORINE-defined agricultural areas. The classes represent agricultural vegetation greenness and provide complementary context for potential agricultural pressure but do not directly quantify irrigation water use or reservoir-specific water withdrawals.

Class	NDVI Range	General Interpretation Within Agricultural Areas
I	−1.00–0.00	Non-vegetated or anomalous pixels, including water, cloud shadow effects, or other residual low-reflectance surfaces within the agricultural mask.
II	0.00–0.20	Very low vegetation greenness, potentially representing bare, fallow, recently cultivated, or harvested agricultural land.
III	0.20–0.40	Low-to-moderate vegetation greenness, potentially associated with sparse, emerging, senescent, or moisture-limited crops.
IV	0.40–0.60	Moderate vegetation greenness and active crop development.
V	0.60–0.80	High vegetation greenness and relatively dense crop canopy.
VI	0.80–1.00	Very high vegetation greenness and dense, vigorous crop canopy.

3. Results

3.1. Long-Term Drought Characteristics and Drought Frequencies

Drought frequency and severity differed among the study basins, providing the long-term hydroclimatic context for interpreting reservoir storage dynamics during 2013–2022 (Figure 3).

The Meriç–Ergene Basin exhibited some of the highest drought frequencies, reaching 19.17% for RDI-12, 16.90% for SPEI-12, and 13.22% for SPI-12. Drought was particularly pronounced at the Edirne, Uzunköprü, and Kırklareli stations, reflecting Thrace's transition between maritime and continental influences (Figure 3a–c). Altınyazı, used for irrigation, and Kırklareli, used for irrigation and drinking water supply, are located within this variable setting. The year 2001 was identified as a critical drought period.

The Susurluk Basin recorded the highest frequency of severe drought (9.38%), while overall frequencies reached 18.71% for RDI-12, 17.00% for SPEI-12, and 14.91% for SPI-12. Drought was more frequent around Bandırma and less frequent around Bursa, reflecting the transition from maritime conditions in the north to increasingly continental conditions in the south and southeast (Figure 3a–c). The years 2007 and 2017 were prominent drought periods relevant to the Doğancı and İkizcetepeler reservoir systems.

The Northern Aegean Basin exhibited moderate drought frequencies of 13.24% for SPI-12, 17.19% for SPEI-12, and 14.37% for RDI-12. The comparatively high SPEI-12 frequency suggests that temperature-dependent atmospheric water demand contributed to regional drought development. Drought was more pronounced around Bayramiç and Çanakkale, where Mediterranean conditions produce strong contrasts between winter precipitation and warm, dry summers (Figure 3a–c). The years 2007 and 2020 were prominent drought periods.

The Marmara Basin recorded frequencies of 17.37% for RDI-12, 16.23% for SPEI-12, and 14.53% for SPI-12. It also exhibited the highest extreme-drought frequency (4.45%) and the lowest RDI value (−6.29). Drought was particularly pronounced around Istanbul, Kocaeli, and Çanakkale (Figure 3a–c). The contrast between Black Sea-influenced areas and the drier sectors of southern Marmara produced substantial within-basin heterogeneity.

Consequently, Ömerli, Terkos, Yuvacık, Bakacak, and Atikhisar may experience different local drought conditions despite being located within the same basin.

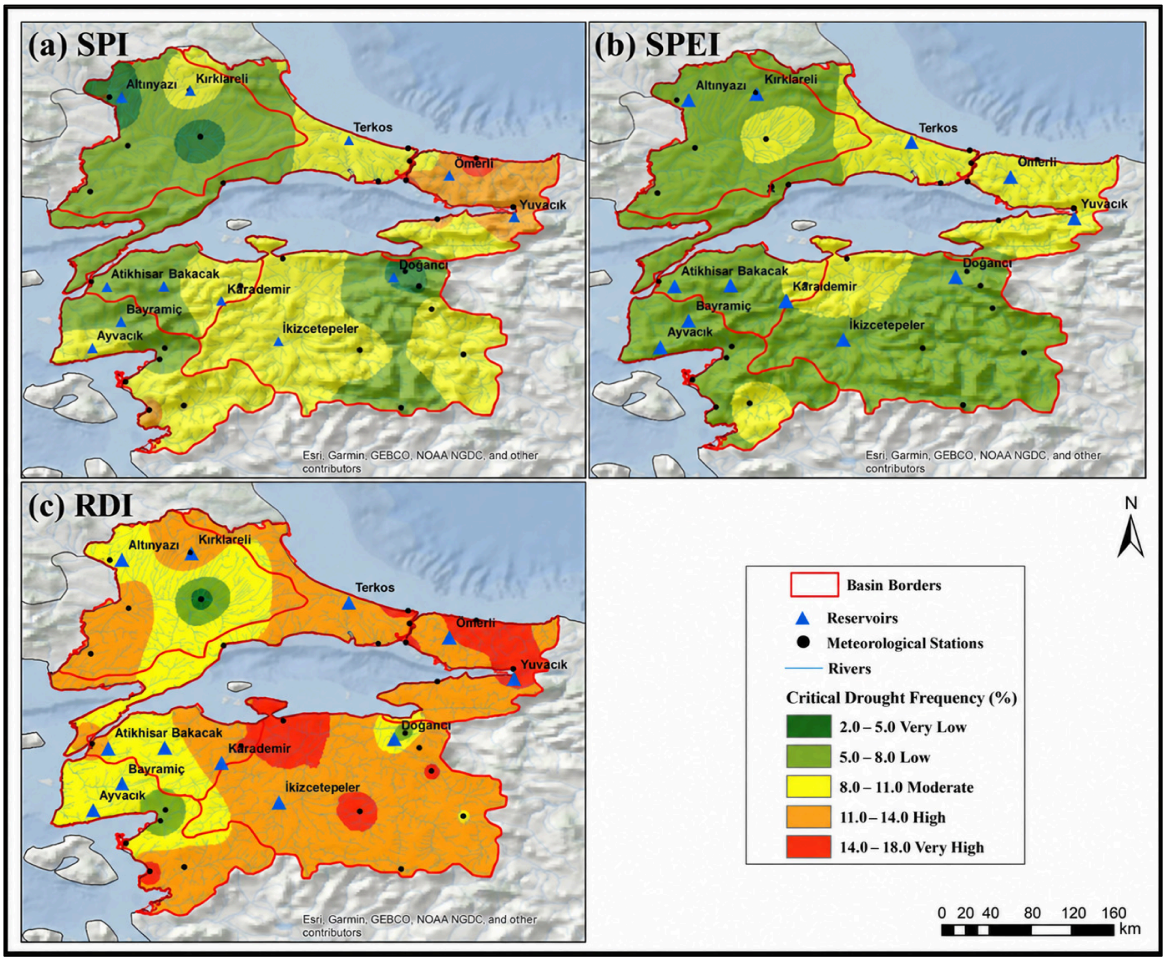


Figure 3. The spatial distribution of the critical drought frequency (%) calculated using the (**a**) SPI, (**b**) SPEI and (**c**) RDI in the Meriç–Ergene, Marmara, Northern Aegean and Susurluk catchment areas. The figure also shows the catchment boundaries, river network, dams and meteorological stations.

Overall, Meriç–Ergene and Susurluk were characterized by relatively high drought frequencies, whereas Marmara experienced the greatest extreme-drought intensity. The station-based maps demonstrate that drought was spatially heterogeneous within individual basins because of topographic and maritime–continental influences (Figure 3a–c). Basin mean indices were therefore retained for regional comparison, while their reservoir-scale robustness was evaluated using locally weighted indices in Section 3.4.

3.2. The Effect of Climatic Forcing on Reservoir Storage Dynamics

Seasonal predictive performance varied substantially among reservoirs under LOYO-CV, with positive skill in 26 of the 48 reservoir–season combinations (Figure 4). The highest performance was obtained for Altınyazı in autumn (RF, R^2 = 0.79). Relatively strong results were also observed for Bakacak and Kırklareli in spring (LM, R^2 = 0.58 for both), Karaidemir in autumn (LM, R^2 = 0.51), Bayramiç in spring (LM, R^2 = 0.51), Terkos in winter (RF, R^2 = 0.50), and Ömerli in winter (RF, R^2 = 0.47). Performance was weaker for Atikhisar in spring (LM, R^2 = 0.35), Doğancı in spring (GAM, R^2 = 0.16), İkizcetepeler in autumn (LM, R^2 = 0.04), and Ayvacık in winter (GAM, R^2 = 0.04). Yuvacık produced a negative R^2 even in its best season (summer; LM, R^2 = −0.09), indicating no improvement over the mean observation benchmark (Figure 4; Table 3).

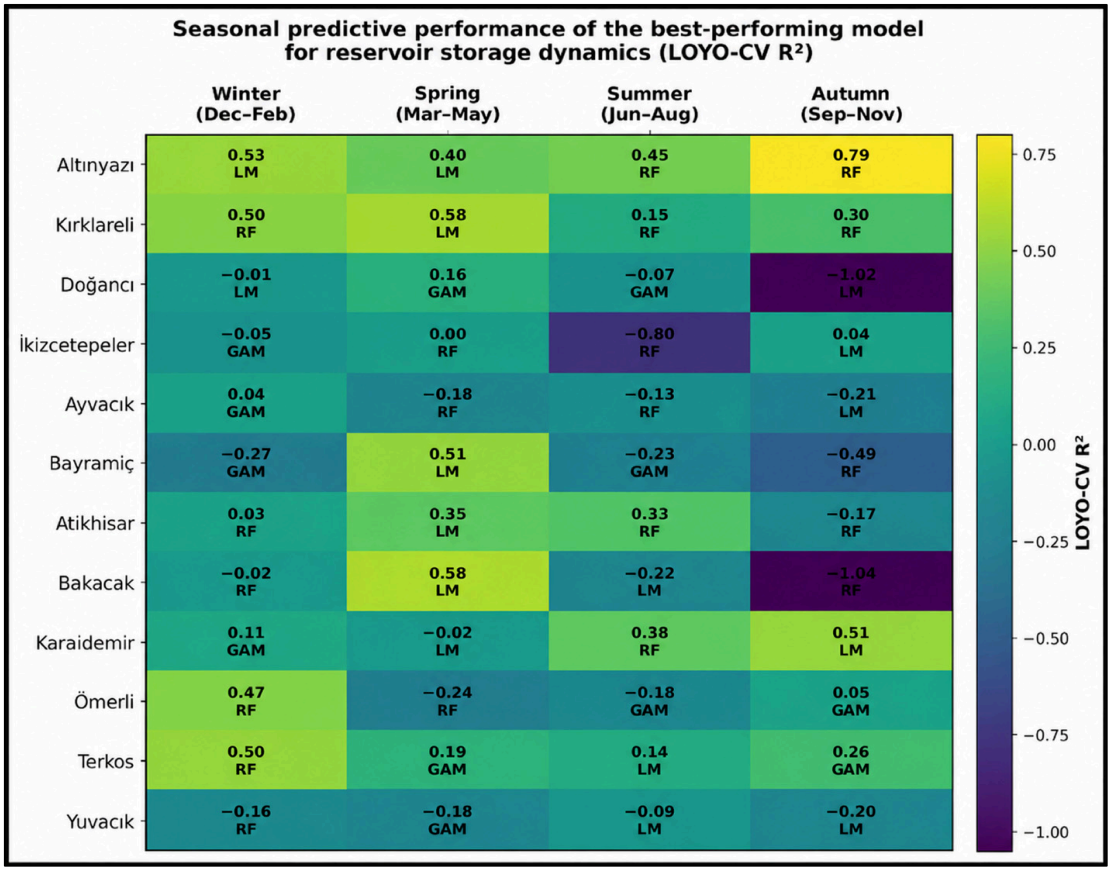


Figure 4. Seasonal variation in the best predictive performance for reservoir storage under leave-one-year-out cross-validation (LOYO-CV), showing the cross-validated R^2 and best performing model for each reservoir–season combination.

Table 3. Best seasonal model performance for reservoir storage based on leave-one-year-out cross-validation (LOYO-CV), including the number of observations (*N*), best performing season and model, cross-validated R^2, and dominant drought predictor for each reservoir.

Reservoir	Purpose	Best Season	Best Model	*N*	LOYO-CV R^2	Dominant Predictor
Altınyazı	Irrigation	Autumn	RF	27	0.79	RDI-9
Kırklareli	Irrigation + Drinking Water	Spring	LM	25	0.58	SPI-6
Doğancı	Drinking Water	Spring	GAM	25	0.16	SPI-6
İkizcetepeler	Irrigation + Drinking Water	Autumn	LM	27	0.04	SPI-6
Ayvacık	Irrigation + Drinking Water	Winter	GAM	28	0.04	SPEI-3
Bayramiç	Irrigation + Hydropower	Spring	LM	26	0.51	SPI-9
Atikhisar	Irrigation + Drinking Water	Spring	LM	27	0.35	RDI-6
Bakacak	Irrigation	Spring	LM	27	0.58	SPEI-12
Karaidemir	Irrigation	Autumn	LM	26	0.51	SPI-12
Ömerli	Drinking Water	Winter	RF	28	0.47	SPI-9
Terkos	Drinking Water	Winter	RF	28	0.50	SPI-12
Yuvacık	Drinking Water	Summer	LM	27	−0.09	SPI-12

Spring was the best performing season for Atikhisar, Bakacak, Bayramiç, Doğancı, and Kırklareli; winter for Ayvacık, Ömerli, and Terkos; and autumn for Altınyazı, İkizcetepeler, and Karaidemir. Summer performed best only for Yuvacık, although its skill remained negative. Thus, no season consistently governed drought–storage relationships across all reservoirs (Figure 4; Table 3).

Across the 48 reservoir–season combinations, RF was the best performing model in 20 cases, compared with 16 for LMs and 12 for GAMs (Figure 5). Positive LOYO-CV R^2 values were obtained in 23 RF models, 19 LMs, and 17 GAMs. Although RF performed best most frequently, no approach was universally superior, and all three produced negative R^2 values in some combinations.

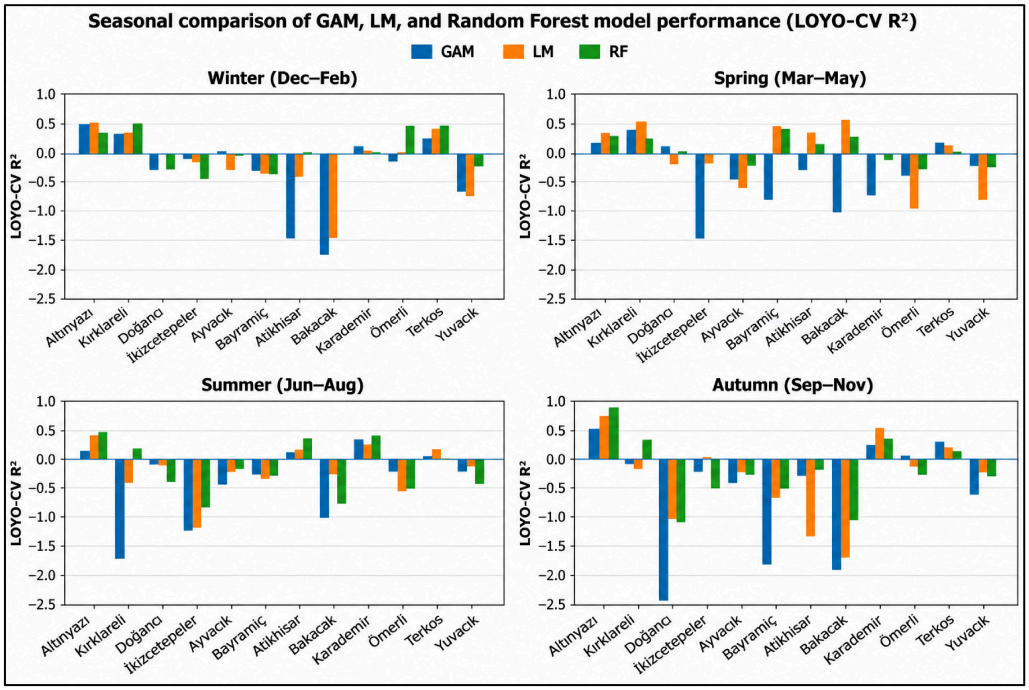


Figure 5. Seasonal comparison of the predictive performance of GAMs, LMs, and RF across the twelve study reservoirs under leave-one-year-out cross-validation (LOYO-CV), expressed as cross-validated R^2.

Predictor selection also varied among reservoirs (Table 3). The dominant predictors were RDI-9 for Altınyazı; RDI-6 for Atikhisar; SPEI-12 for Bakacak; SPEI-3 for Ayvacık; SPI-9 for Bayramiç and Ömerli; SPI-6 for Doğancı, İkizcetepeler, and Kırklareli; and SPI-12 for Karaidemir, Terkos, and Yuvacık. Overall, 6–12-month indices were dominant for 11 of the 12 reservoirs, indicating the importance of cumulative hydroclimatic conditions.

Regression-based inference was evaluated separately from predictive performance. A total of 9 out of 143 selected LM coefficients remained significant after BH-FDR correction, primarily for 6- and 12-month indices in Altınyazı, Bakacak, İkizcetepeler, Karaidemir, and Kırklareli. Residual autocorrelation occurred in 27 of 48 LMs, and variance inflation factor values exceeded 5 in 25 models. Because predictor selection and inference used the same datasets, the FDR-adjusted coefficients were treated as exploratory rather than confirmatory.

Overall, LOYO-CV provided a conservative assessment: predictive performance was moderate to strong for some reservoir–season combinations but weak or negative for others. The frequent selection of 6–12-month indices indicates the importance of cumulative drought, while differences among RF, GAMs, and LMs confirm that predictive skill was reservoir- and season-specific (Figures 4 and 5; Table 3).

3.3. Agricultural Vegetation Dynamics and Their Contextual Relevance to Reservoir Storage

The growing season NDVI showed temporal and spatial variability across agricultural areas in the four basins during 2013–2022 (Figures 6 and 7). Because forests and other non-agricultural classes were excluded, the results represent April–September agricultural

vegetation activity rather than total basin vegetation. Marmara consistently recorded the highest values, increasing from 0.48 in 2013 to 0.55 in 2018 and reaching 0.53 in 2022. Susurluk increased from 0.43 to 0.51 and subsequently declined to 0.49. Meriç–Ergene rose from 0.45 in 2013 to 0.51 in 2014, fell to 0.43 in 2016, and reached 0.47 in 2022. Northern Aegean generally recorded the lowest NDVI, ranging between 0.43 and 0.48 and reaching 0.45 in 2022 (Figure 6).

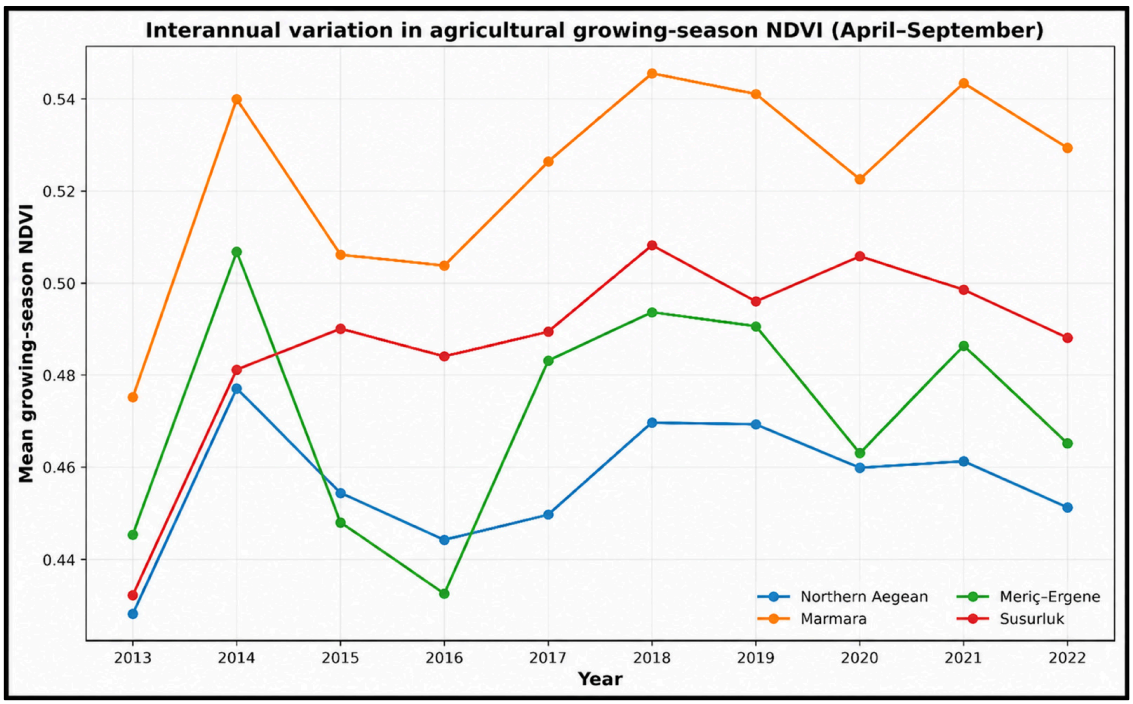


Figure 6. Interannual variation in the mean growing season (April–September) NDVI across agricultural areas of the Meriç–Ergene, Marmara, Northern Aegean, and Susurluk basins during 2013–2022. Forests and other non-agricultural land cover classes were excluded.

Basin means remained predominantly within the 0.40–0.60 range, indicating moderate growing season greenness in agricultural areas. None exceeded 0.60 after forests, wetlands, grasslands, settlements, and other non-agricultural classes were excluded, reducing the upward bias associated with dense natural vegetation.

The 2013 and 2022 maps showed a broadly similar spatial pattern but substantial local differences (Figure 7a,b). The endpoint difference, calculated as $NDVI_{2022} - NDVI_{2013}$, was positive on average in all basins: 0.020 in Meriç–Ergene, 0.023 in Northern Aegean, 0.054 in Marmara, and 0.056 in Susurluk. However, positive and negative pixels coexisted within each basin, demonstrating spatial heterogeneity (Figure 7c). These differences compare two endpoint years rather than representing a continuous trend and may reflect hydroclimatic variability, crop rotation, agricultural management, and irrigation conditions.

Crop and irrigated-area information provided additional context. Reported cultivation areas included approximately 7730 ha of rice associated with Altınyazı, 11,840 ha around Karaidemir, and 9100 ha around Bakacak; 15,800 ha of silage maize around Bayramiç; 9050 ha around Kırklareli; 5200 ha of maize around Atikhisar; 1700 ha of silage maize around İkizcetepeler; and 3900 ha of alfalfa around Ayvacık. These crops may generate substantial seasonal irrigation requirements, but the reported areas and the NDVI do not quantify withdrawals from individual reservoirs.

Seasonal modeling likewise showed reservoir-specific responses. Spring performed best for Kırklareli, Doğancı, Bayramiç, Atikhisar, and Bakacak; autumn for Altınyazı, İkizcetepeler, and Karaidemir; winter for Ayvacık, Ömerli, and Terkos; and summer for

Yuvacık (Figure 4; Table 3). Although spring and autumn performance may coincide with growing season demand and recharge, these associations do not demonstrate irrigation-related causation.

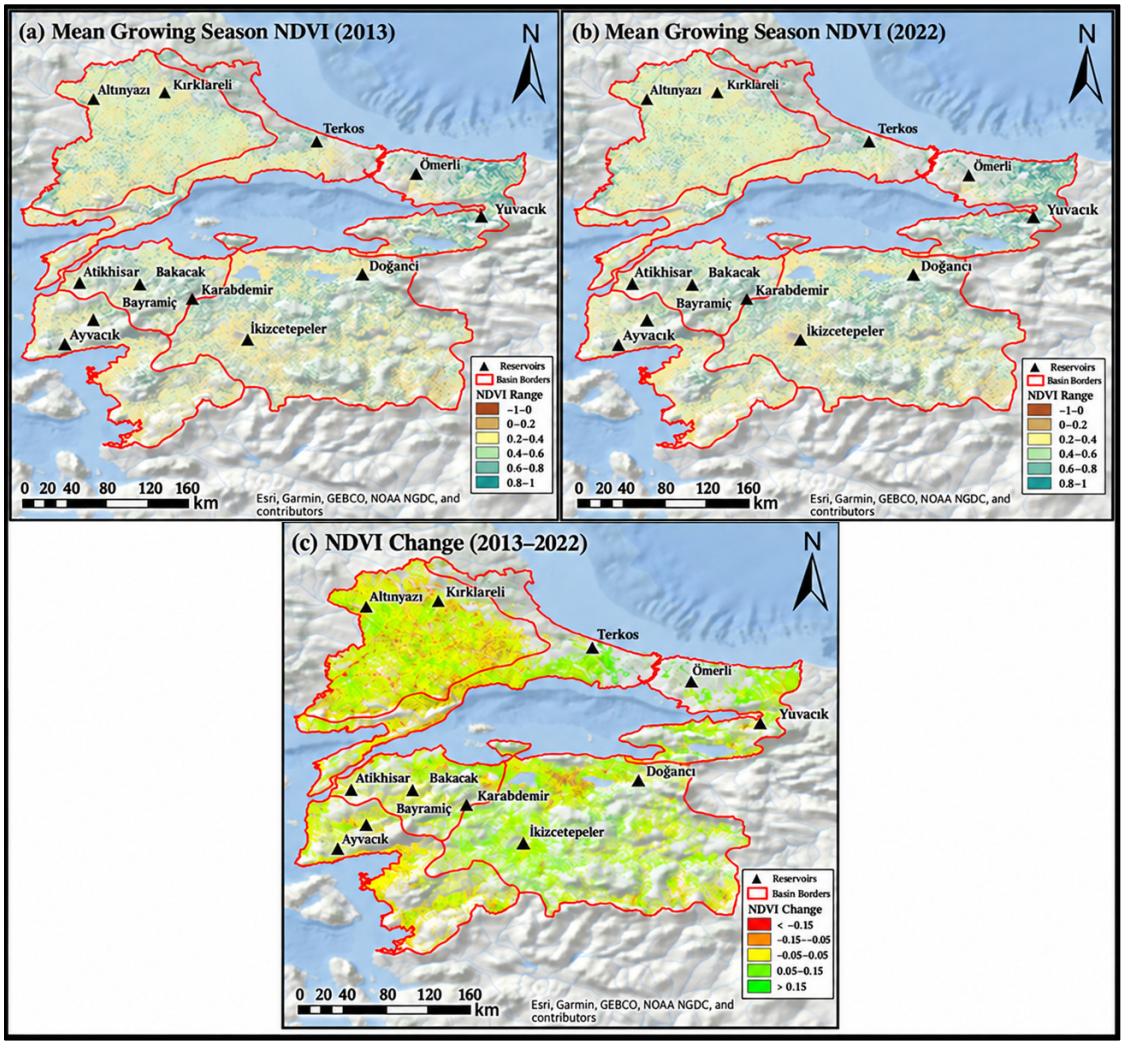


Figure 7. The spatial distribution of the mean growing season (April–September) NDVI in agricultural areas in 2013 (**a**) and 2022 (**b**) and the NDVI difference between the two years (2022 − 2013) (**c**) across the study basins of northwestern Türkiye. Forests and other non-agricultural land cover classes were excluded. Positive and negative values indicate increases and decreases in vegetation greenness, respectively.

Overall, the agricultural NDVI increased between the two endpoint years, but spatial and interannual patterns differed among basins. The NDVI, crop characteristics, and reservoir purpose therefore provide complementary context for interpreting reservoir responses alongside drought conditions but cannot separate climatic effects from reservoir-specific water use.

3.4. Sensitivity to the Spatial Representation of Drought

Basin mean and reservoir local drought series showed strong agreement across the 180 reservoir–index combinations, with a mean correlation of 0.88 and a median of 0.89. Correlations ranged from 0.66 to 0.99, and 83 comparisons reached at least 0.90. Basin averaging therefore captured the broad regional drought signal, although local differences remained.

Replacing basin mean indices with Local-IDW indices did not systematically improve out-of-sample performance. Across the twelve reservoirs, the mean and median changes in

the best LOYO-CV R^2 were −0.02 and −0.03, respectively (Figure 8a). Local-IDW improved performance for five reservoirs but reduced it for seven. The largest improvements occurred for İkizcetepeler (0.04 to 0.46) and Atikhisar (0.35 to 0.64), followed by Yuvacık (−0.09 to 0.15), Bayramiç (0.51 to 0.62), and Bakacak (0.58 to 0.69). Conversely, performance declined markedly for Doğancı (0.16 to −0.32), Karaidemir (0.51 to 0.12), and Altınyazı (0.79 to 0.56).

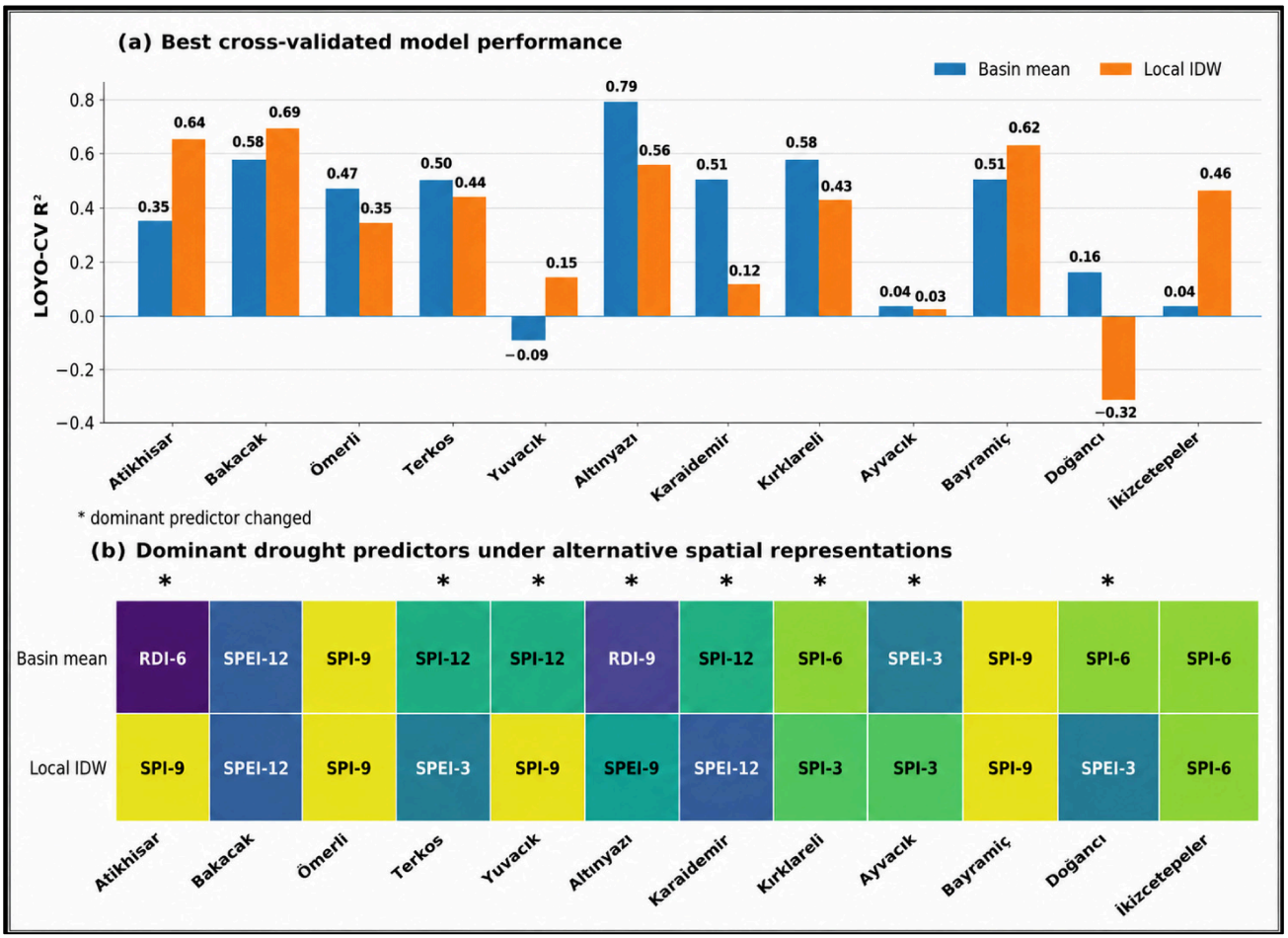


Figure 8. The sensitivity of reservoir drought–storage relationships to the spatial representation of drought. (**a**) Comparison of the best LOYO-CV R^2 values obtained using basin mean and Local-IDW drought indices. (**b**) Comparison of dominant drought predictors between the two spatial representations; asterisks indicate reservoirs where the dominant predictor changed.

Spatial representation also affected predictor identification (Figure 8b). The dominant predictor remained unchanged in four reservoirs—SPEI-12 for Bakacak, SPI-9 for Bayramiç and Ömerli, and SPI-6 for İkizcetepeler—but changed in eight. Notable changes included RDI-9 to SPEI-9 for Altınyazı, RDI-6 to SPI-9 for Atikhisar, SPI-6 to SPEI-3 for Doğancı, and SPI-12 to SPEI-12 for Karaidemir. Changes also occurred for Kırklareli, Terkos, Yuvacık, and Ayvacık, although some Local-IDW models selected several predictors with equal frequency. The best performing season remained unchanged in nine reservoirs and changed only for Atikhisar, Doğancı, and Yuvacık.

Overall, basin means were appropriate for the primary regional comparison, but local hydroclimatic variability affected predictive performance and dominant-predictor selection for individual reservoirs. The predictors reported in Table 3 should therefore be interpreted as prevailing signals under the basin mean representation rather than as spatially invariant controls. Local-IDW results complement rather than replace the primary analysis.

4. Discussion

Reservoir storage responses to hydroclimatic drought in northwestern Türkiye depended strongly on accumulation timescale and reservoir-specific conditions. In the best seasonal models, 6–12-month indices were dominant for 11 of the 12 reservoirs, indicating stronger associations with cumulative hydroclimatic conditions than with short-term anomalies. These responses may integrate antecedent precipitation deficits, soil moisture, groundwater recharge, runoff, and delayed catchment inflows. This role of hydrological memory agrees with Katipoğlu et al. [64] and previous studies emphasizing cumulative controls on reservoir and hydrological drought dynamics [25,38,52,53].

The importance of the SPI, SPEI, and RDI differed among reservoirs, confirming that no single indicator represented all drought–storage relationships. The SPI was most frequently dominant under the basin mean representation, while the selection of the SPEI and RDI for several reservoirs suggests that temperature-dependent atmospheric water demand may also contribute to reservoir sensitivity under Mediterranean conditions. Rising temperature and evapotranspiration can intensify precipitation deficits and reduce water availability and catchment recharge [3,5]. Nevertheless, dominant predictors represent the prevailing signals under the applied screening and spatial representation rather than exclusive physical controls.

Seasonal performance also varied considerably. Spring performed best for several reservoirs, while autumn and winter were more informative for others; Yuvacık produced negative predictive skill even in its best season. These findings indicate that no season uniformly controls reservoir responses and are consistent with previous studies emphasizing hydrological memory, climatic variability, operational controls, and nonlinear modelling of reservoir and drought dynamics [17,64–68]. LOYO-CV produced a substantially more conservative assessment than model goodness-of-fit alone and demonstrated that apparently strong in-sample relationships may not provide reliable out-of-sample prediction.

RF, GAMs, and LMs provided complementary results. RF performed best most frequently, but LMs and GAMs outperformed it in several reservoir–season combinations, and all approaches produced negative R^2 values in some cases. Only 9 of 143 post-selection LM terms remained significant after BH-FDR correction. Because inference followed predictor selection and diagnostic tests identified residual autocorrelation and multicollinearity in some LMs, these relationships should be considered exploratory. Statistical significance and out-of-sample predictive skill therefore represent complementary rather than interchangeable evidence.

Reservoirs within the same basin responded differently to similar drought conditions, reflecting variations in local climate, catchment properties, recharge, land cover, reservoir function, and operating practices. Reservoirs should therefore be understood as hydrogeographic systems in which climatic, catchment, and management processes interact rather than as passive systems responding uniformly to basin-scale forcing [4,16,66]. This interpretation agrees with research on Atikhisar Reservoir, where surface-area changes could not be explained solely by meteorological drought despite associations with the SPI and SPEI [69].

The spatial sensitivity analysis reinforced this interpretation. Basin mean and Local-IDW series were strongly correlated, confirming that basin averages represented the broad regional drought signal. However, Local-IDW did not systematically improve predictive performance: it improved five reservoirs but reduced seven, while the dominant predictor changed in eight. The contrasting changes observed for Atikhisar, İkizcetepeler, Altınyazı, and Doğancı demonstrate that local representation may substantially alter individual results even when basin-level agreement is strong. Basin means are therefore suitable for regional comparison, but dominant predictors should be interpreted as representation-dependent

rather than spatially invariant controls. This conclusion is consistent with the geographic and hydroclimatic variability reported across the study region [11,38–42,53,58,59].

The revised NDVI analysis provided complementary evidence of agricultural vegetation dynamics. Restricting the analysis to CORINE agricultural classes produced lower and more representative agricultural NDVI values than the previous whole-basin assessment, which had been influenced by dense natural vegetation. Marmara maintained the highest agricultural NDVI, while Northern Aegean generally recorded the lowest values. The 2013–2022 endpoint comparison indicated positive mean changes in all basins, but positive and negative pixels coexisted, demonstrating substantial spatial heterogeneity. Because the map compares two endpoint years, these differences should not be interpreted as a continuous temporal trend.

The NDVI represents vegetation greenness rather than water withdrawal, and agricultural pixels within basin polygons cannot be assigned directly to individual reservoir command areas. Observed NDVI differences may reflect hydroclimatic variability, crop rotation, irrigation conditions, and agricultural management. Accordingly, the NDVI was used as contextual evidence rather than a quantitative proxy for abstraction. Remote sensing remains valuable when evaluated jointly with drought indicators and interpreted within its spatial and hydrological limitations [38,60–63]. Previous research has demonstrated that remote sensing can reveal spatial–temporal changes in reservoir areas associated with meteorological drought [69]. Machine-learning approaches have also been used to evaluate water scarcity under combined climate-change and population scenarios [70], while reservoir operation can alter drought impacts under changing climatic conditions [71]. At agricultural and basin scales, Landsat-based drought monitoring, vegetation-response analysis, land-use and land-cover assessment, and multi-index approaches provide complementary evidence of drought effects [72–75]. These issues are especially important for irrigation systems because sustainable irrigation expansion is constrained by water-storage availability [76], while agricultural water-supply reliability depends on reservoir operation under uncertain precipitation and upstream runoff conditions [77]. At broader scales, previous studies have documented drought-related reservoir fullness fluctuations [78], the contribution of municipal and agricultural demand to future water shortages [79], the global sensitivity of water storage to hydroclimatic variability [80] and the value of GIS-based multivariate indices for hydrogeological drought management [81].

Water-demanding crops such as rice, maize, silage maize, and alfalfa occur in agricultural areas associated with Altınyazı, Karaidemir, Bakacak, Bayramiç, Kırklareli, Atikhisar, İkizcetepeler, and Ayvacık. These crops may generate substantial seasonal irrigation requirements and influence reservoir–storage relationships during the growing season. This interpretation is supported by previous observations from Bayramiç Dam Lake, where irrigation and other managed water releases were shown to contribute substantially to reservoir outflows, whereas hydro-meteorological conditions primarily controlled water inputs [42]. However, command-area boundaries and reservoir-specific withdrawal records were unavailable; climatic and agricultural contributions could therefore not be quantitatively separated. Differences among reservoirs should consequently be interpreted as associations with agricultural context and reservoir function rather than as direct causal effects of irrigation withdrawals [36,37,42,58,62,64,65].

A similar limitation applies to drinking water reservoirs. Ömerli, Terkos, Yuvacık, and Doğancı may be affected by municipal demand, transfers, and operational decisions in addition to hydroclimatic recharge. Yuvacık was a notable outlier, with negative cross-validated R^2 values in all four seasons. This weak predictive skill may reflect the influence of unmodeled operational factors, including municipal withdrawals, inter-system transfers, and reservoir management decisions, although the available data do not allow these

effects to be quantified separately. Because consistent reservoir-specific population and municipal demand data were unavailable, these influences were not explicitly modeled. Drinking water reservoirs therefore cannot be treated as climate-only reference systems, and reservoir purpose differences do not demonstrate that irrigation reservoirs are inherently more drought-sensitive. Furthermore, because forests were excluded from the revised dataset, agricultural NDVI values should not be attributed to protected forest catchments. Future studies incorporating irrigation and municipal withdrawals, inflows, releases, transfers, and operating rules could separate climatic and anthropogenic contributions more directly [4,15,41,78].

Overall, reservoir storage variability reflects cumulative drought effects together with seasonal, spatial, and reservoir-specific heterogeneity. The common LOYO-CV framework provides a conservative assessment of predictive performance, while fold-specific screening, BH-FDR correction, and Local-IDW sensitivity analysis improve the reliability of interpretation. The agricultural NDVI, crop characteristics, reservoir purpose, and irrigated area provide relevant context but do not permit causal attribution of storage changes to human water use. The integrated framework therefore supports reservoir-specific drought assessment without assigning observed variability exclusively to climatic or anthropogenic forcing [6,38,67–69].

5. Conclusions

This study evaluated reservoir storage responses to hydroclimatic drought in northwestern Türkiye using the SPI, SPEI, and RDI together with RF, GAMs, and LMs. Drought indices at 6–12-month scales were dominant in the best seasonal models for 11 of the 12 reservoirs, indicating the importance of cumulative hydroclimatic conditions. However, predictive performance varied substantially among reservoirs and seasons, demonstrating that no single index, timescale, season, or model represented all reservoir responses.

LOYO-CV provided a conservative assessment of out-of-sample performance. RF performed best in 20 of the 48 reservoir–season combinations, compared with 16 for LMs and 12 for GAMs, but no approach was universally superior. Only 9 of 143 post-selection LM terms remained significant after BH-FDR correction. These relationships were treated as exploratory, confirming that statistical significance and predictive performance provide complementary rather than interchangeable evidence.

Basin mean and Local-IDW drought series were strongly correlated (mean $r = 0.88$; median $r = 0.89$), but local representation did not systematically improve prediction. Nevertheless, changes in dominant predictors for eight reservoirs demonstrated that local hydroclimatic heterogeneity can influence reservoir-specific interpretations.

The agricultural-area NDVI, reservoir function, irrigated area, and crop characteristics provided contextual information but did not quantify reservoir withdrawals. Because command-area boundaries, irrigation withdrawals, and consistent municipal demand data were unavailable, the results do not demonstrate anthropogenic causation, and drinking water reservoirs cannot be considered climate-only reference systems.

Overall, reservoir drought sensitivity reflects cumulative drought effects and pronounced seasonal, spatial, and reservoir-specific variability. The common cross-validation, multiple-testing correction, and spatial sensitivity framework provides a rigorous basis for reservoir-specific assessment. Future studies incorporating inflows, releases, irrigation and municipal withdrawals, transfers, operating rules, and command-area boundaries could distinguish climatic and anthropogenic controls more directly and support adaptive reservoir management.

Author Contributions: F.Y.Ö.: writing (original draft), visualization, validation, software, formal analysis, investigation, resources, data curation; E.E.: review and editing of the manuscript, visual-

ization, validation, software, formal analysis, investigation, resources, data curation; E.Ö.: review and editing of the manuscript, conceptualization, methodology, validation, supervision, project administration, resources; H.T.: review and editing of the manuscript, methodology, supervision; M.K.: review and editing of the manuscript, methodology, supervision. All authors have read and agreed to the published version of the manuscript.

Funding: This research received no external funding.

Data Availability Statement: The raw data supporting the conclusions of this article will be made available by the authors on request.

Acknowledgments: The reservoir data used in this study were obtained within the scope of Project No. 4771, supported by the Scientific Research Projects Coordination Unit of Çanakkale Onsekiz Mart University (Project Years: 2024–2025).

Conflicts of Interest: The authors declare no conflicts of interest.

References

1. Wanders, N.; Wada, Y. Human and Climate Impacts on the 21st Century Hydrological Drought. *J. Hydrol.* **2015**, *526*, 208–220. [CrossRef]
2. AghaKouchak, A.; Chiang, F.; Huning, L.S.; Love, C.A.; Mallakpour, I.; Mazdiyasni, O.; Moftakhari, H.; Papalexiou, S.M.; Ragno, E.; Sadegh, M. Climate Extremes and Compound Hazards in a Warming World. *Annu. Rev. Earth Planet. Sci.* **2020**, *48*, 519–548. [CrossRef]
3. Ciampittiello, M.; Marchetto, A.; Boggero, A. Water Resources Management under Climate Change: A Review. *Sustainability* **2024**, *16*, 3590. [CrossRef]
4. Biemans, H.; Haddeland, I.; Kabat, P.; Ludwig, F.; Hutjes, R.W.A.; Heinke, J.; Von Bloh, W.; Gerten, D. Impact of Reservoirs on River Discharge and Irrigation Water Supply during the 20th Century. *Water Resour. Res.* **2011**, *47*, 2009WR008929. [CrossRef]
5. Simeone, C.E.; Hammond, J.C.; Archfield, S.A.; Broman, D.; Condon, L.E.; Eldardiry, H.; Olson, C.G.; Steyaert, J.C. Declining Reservoir Reliability and Increasing Reservoir Vulnerability: Long-Term Observations Reveal Longer and More Severe Periods of Low Reservoir Storage for Major United States Reservoirs. *Geophys. Res. Lett.* **2024**, *51*, e2024GL109476. [CrossRef]
6. Yassin, A.; Ricci, G.F.; Gentile, F.; Girolamo, A.M.D. Benefits and Challenges of Small Dams in Mediterranean Climate Region: A Review. *Hydrology* **2025**, *13*, 10. [CrossRef]
7. Siltu, E.; Hatipoglu, A.M.; Kumcu, S.Y.; Selek, B. Role of Dams on Climate Change Adaptation, Mitigation and Resilience. In *Hydrology and Urban Water Supply*; Bahadir, A.M., Haarstrick, A., Karadirek, I.E., Aydin, M.E., Kumcu, S.Y., Bandyopadhyay, A., Eds.; Water and Wastewater Management; Springer Nature Switzerland: Cham, Switzerland, 2024; pp. 77–85, ISBN 978-3-031-72588-3.
8. Van Loon, A.F.; Gleeson, T.; Clark, J.; Van Dijk, A.I.J.M.; Stahl, K.; Hannaford, J.; Di Baldassarre, G.; Teuling, A.J.; Tallaksen, L.M.; Uijlenhoet, R.; et al. Drought in the Anthropocene. *Nat. Geosci.* **2016**, *9*, 89–91. [CrossRef]
9. Vicente-Serrano, S.M.; Beguería, S.; López-Moreno, J.I. A Multiscalar Drought Index Sensitive to Global Warming: The Standardized Precipitation Evapotranspiration Index. *J. Clim.* **2010**, *23*, 1696–1718. [CrossRef]
10. Zarei, A.R.; Shabani, A.; Moghimi, M.M. Accuracy Assessment of the SPEI, RDI and SPI Drought Indices in Regions of Iran with Different Climate Conditions. *Pure Appl. Geophys.* **2021**, *178*, 1387–1403. [CrossRef]
11. Oduor, B.O.; Martínez-Pérez, S.; Rodríguez-Castellanos, J.M.; Sánchez-Gómez, A.; Molina-Navarro, E. Future of Water Security in Mediterranean Reservoirs: Advancing SWAT + Modeling of Hydrological Response To Climate Change in Central Spain. *Earth Syst. Environ.* **2026**. [CrossRef]
12. Mishra, A.K.; Singh, V.P. A Review of Drought Concepts. *J. Hydrol.* **2010**, *391*, 202–216. [CrossRef]
13. Serkendiz, H.; Tatli, H.; Kılıç, A.; Çetin, M.; Sungur, A. Analysis of Drought Intensity, Frequency and Trends Using the Spei in Turkey. *Theor. Appl. Climatol.* **2024**, *155*, 2997–3012. [CrossRef]
14. Naderi, M. Assessment of Water Security under Climate Change for the Large Watershed of Dorudzan Dam in Southern Iran. *Hydrogeol. J.* **2020**, *28*, 1553–1574. [CrossRef]
15. Mirdashtvan, M.; Najafinejad, A.; Malekian, A.; Sa'doddin, A. Sustainable Water Supply and Demand Management in Semi-Arid Regions: Optimizing Water Resources Allocation Based on RCPs Scenarios. *Water Resour. Manag.* **2021**, *35*, 5307–5324. [CrossRef]
16. Wang, D.; Hejazi, M. Quantifying the Relative Contribution of the Climate and Direct Human Impacts on Mean Annual Streamflow in the Contiguous United States. *Water Resour. Res.* **2011**, *47*, 2010WR010283. [CrossRef]
17. Ehsani, N.; Vörösmarty, C.J.; Fekete, B.M.; Stakhiv, E.Z. Reservoir Operations under Climate Change: Storage Capacity Options to Mitigate Risk. *J. Hydrol.* **2017**, *555*, 435–446. [CrossRef]

18. Zeff, H.B.; Herman, J.D.; Reed, P.M.; Characklis, G.W. Cooperative Drought Adaptation: Integrating Infrastructure Development, Conservation, and Water Transfers into Adaptive Policy Pathways. *Water Resour. Res.* **2016**, *52*, 7327–7346. [CrossRef]
19. Vicente-Serrano, S.M.; Azorin-Molina, C.; Sanchez-Lorenzo, A.; Revuelto, J.; Morán-Tejeda, E.; López-Moreno, J.I.; Espejo, F. Sensitivity of Reference Evapotranspiration to Changes in Meteorological Parameters in S Pain (1961–2011). *Water Resour. Res.* **2014**, *50*, 8458–8480. [CrossRef]
20. Tigkas, D.; Vangelis, H.; Tsakiris, G. Drought Characterisation Based on an Agriculture-Oriented Standardised Precipitation Index. *Theor. Appl. Climatol.* **2019**, *135*, 1435–1447. [CrossRef]
21. Jabbi, F.F.; Li, Y.; Zhang, T.; Bin, W.; Hassan, W.; Songcai, Y. Impacts of Temperature Trends and SPEI on Yields of Major Cereal Crops in the Gambia. *Sustainability* **2021**, *13*, 12480. [CrossRef]
22. Matiu, M.; Ankerst, D.P.; Menzel, A. Interactions between Temperature and Drought in Global and Regional Crop Yield Variability during 1961–2014. *PLoS ONE* **2017**, *12*, e0178339. [CrossRef] [PubMed]
23. Peña-Gallardo, M.; Vicente-Serrano, S.M.; Domínguez-Castro, F.; Beguería, S. The Impact of Drought on the Productivity of Two Rainfed Crops in Spain. *Nat. Hazards Earth Syst. Sci.* **2019**, *19*, 1215–1234. [CrossRef]
24. Torelló-Sentelles, H.; Franzke, C.L.E. Drought Impact Links to Meteorological Drought Indicators and Predictability in Spain. *Hydrol. Earth Syst. Sci.* **2022**, *26*, 1821–1844. [CrossRef]
25. Li, Z.; Huang, S.; Wang, Y.; Zhou, S.; Huang, Q.; Liu, D.; Leng, G. A Process-Oriented Framework to Decipher Drought Propagation Dynamics from Meteorological to Ecological, Agricultural, Hydrological, and Socioeconomic Drought in the Yellow River Basin. *Ecol. Indic.* **2026**, *182*, 114574. [CrossRef]
26. Chen, J.; Shi, H.; Sivakumar, B.; Peart, M.R. Population, Water, Food, Energy and Dams. *Renew. Sustain. Energy Rev.* **2016**, *56*, 18–28. [CrossRef]
27. Pande, S.; Sivapalan, M. Progress in Socio-hydrology: A Meta-analysis of Challenges and Opportunities. *WIREs Water* **2017**, *4*, e1193. [CrossRef]
28. Karaman, M.; Budakoğlu, M.; Uca Avci, Z.D.; Ozelkan, E.; Bulbul, A.; Civas, M.; Tasdelen, S. Determination of Seasonal Changes in Wetlands Using CHRIS/Proba Hyperspectral Satellite Images: A Case Study from Acigöl (Denizli), Turkey. *J. Environ. Biol.* **2015**, *36*, 73–83. [PubMed]
29. García-Ruiz, J.M.; López-Moreno, J.I.; Vicente-Serrano, S.M.; Lasanta–Martínez, T.; Beguería, S. Mediterranean Water Resources in a Global Change Scenario. *Earth-Sci. Rev.* **2011**, *105*, 121–139. [CrossRef]
30. Lionello, P.; Scarascia, L. The Relation between Climate Change in the Mediterranean Region and Global Warming. *Reg. Environ. Change* **2018**, *18*, 1481–1493. [CrossRef]
31. Gorguner, M.; Kavvas, M.L. Modeling Impacts of Future Climate Change on Reservoir Storages and Irrigation Water Demands in a Mediterranean Basin. *Sci. Total Environ.* **2020**, *748*, 141246. [CrossRef] [PubMed]
32. Berhail, S.; Katipoğlu, O.M. Exploring Hydrological and Meteorological Drought Trends in Northeast Algeria: Implications for Water Resource Management. *Theor. Appl. Climatol.* **2024**, *155*, 9689–9712. [CrossRef]
33. Montaldo, N.; Sirigu, S.; Zucca, R.; Ruiu, A.; Corona, R. Hydrological Sustainability of Dam-Based Water Resources in a Mediterranean Basin Undergoing Climate Change. *Hydrology* **2024**, *11*, 200. [CrossRef]
34. Öz, F.Y.; Özelkan, E.; Tatlı, H. Comparative Analysis of SPI, SPEI, and RDI Indices for Assessing Spatio-Temporal Variation of Drought in Türkiye. *Earth Sci. Inform.* **2024**, *17*, 4473–4505. [CrossRef]
35. Özelkan, E.; Karaman, M. Analysis of the Effects of Meteorological and Hydrological Drought in Reservoir Lakes Using Multitemporal Satellite Images: The Case of the Atikhisar Dam (Çanakkale). *Ömer Halisdemir Univ. J. Eng. Sci.* **2018**. [CrossRef]
36. Özelkan, E. Assessment of Temporal Changes in a Reservoir Area Identified by Remote Sensing in Relation to Meteorological Drought: The Case of the Atikhisar Dam (Çanakkale). *Turk. J. Agric. Nat. Sci.* **2019**, *6*, 904–916. [CrossRef]
37. Akgün, S.; Özelkan, E.; Serkendiz, H.; Eren, E.; Karaman, M.; Tatlı, H. Assessing Areal and Volumetric Reservoir Dynamics Using Remote Sensing and In-Situ Measurements to Explore Drought Relationships in the Marmara Region of Türkiye. *Environ. Earth Sci.* **2026**, *85*, 254. [CrossRef]
38. Yıldırım, P. Interannual Variability of Reservoir Occupancy: A Multi-Reservoir Assessment from Çanakkale, Türkiye. *Acta Nat. Sci.* **2026**, 54–64. [CrossRef]
39. Bobat, A. Reasons and Results of Water Shortage in Turkey: The Case Study of Kocaeli. In Proceedings of the Τηεμε B: Urban Water Management, Chania, Crete, Greece, 1 June 2016.
40. Özdemir, A. Assessment of the Effects of Climate Change on Runoff and Sediment Load at the Watershed Scale: The Yuvacık Reservoir Watershed. *J. Geol. Eng.* **2021**, *45*, 129–154. [CrossRef]
41. Doğan, C.; Taş, İ. Availability of Irrigation Water Diverted to Irrigation Areas: The Case of the Bakacık Dam in Çanakkale-Biga. *Turk. J. Agric. Nat. Sci.* **2024**, *11*, 463–474. [CrossRef]
42. Karaman, M.; Özelkan, E. Comparative Assessment of Remote Sensing–Based Water Dynamic in a Dam Lake Using a Combination of Sentinel-2 Data and Digital Elevation Model. *Environ. Monit. Assess.* **2022**, *194*, 92. [CrossRef] [PubMed]

43. Mosavi, A.; Ozturk, P.; Chau, K. Flood Prediction Using Machine Learning Models: Literature Review. *Water* **2018**, *10*, 1536. [CrossRef]
44. Ahmed, A.A.; Sayed, S.; Abdoulhalik, A.; Moutari, S.; Oyedele, L. Applications of Machine Learning to Water Resources Management: A Review of Present Status and Future Opportunities. *J. Clean. Prod.* **2024**, *441*, 140715. [CrossRef]
45. Baltacı, H.; Göktürk, O.M.; Kındap, T.; Ünal, A.; Karaca, M. Atmospheric Circulation Types in Marmara Region (NW Turkey) and Their Influence on Precipitation. *Int. J. Climatol.* **2015**, *35*, 1810–1820. [CrossRef]
46. Sensoy, S.; Demircan, M.; Ulupınar, U.; Balta, I. *Climate of Turkey*; Turkish State Meteorological Service (DMİ): Ankara, Turkey, 2008.
47. Özdin, M. *Analysis of the Effects of Climate Change on Precipitation in the Susurluk Basin Using Artificial Neural Networks*; T.C. Sakarya University Of Applied Sciences Institute Of Graduate Studies: Serdivan, Turkey, 2019.
48. McKee, T.B.; Doesken, N.J.; Kleist, J. The Relationship of Drought Frequency and Duration to Time Scales. In Proceedings of the 8th Conference on Applied Climatology, Anaheim, CA, USA, 17–22 January 1993.
49. Türkeş, M.; Tatlı, H. Use of the Standardized Precipitation Index (SPI) and a Modified SPI for Shaping the Drought Probabilities over Turkey. *Int. J. Climatol.* **2009**, *29*, 2270–2282. [CrossRef]
50. Danandeh Mehr, A.; Sorman, A.U.; Kahya, E.; Hesami Afshar, M. Climate Change Impacts on Meteorological Drought Using SPI and SPEI: Case Study of Ankara, Turkey. *Hydrol. Sci. J.* **2020**, *65*, 254–268. [CrossRef]
51. Ndayiragije, J.M.; Li, F. Effectiveness of Drought Indices in the Assessment of Different Types of Droughts, Managing and Mitigating Their Effects. *Climate* **2022**, *10*, 125. [CrossRef]
52. Tsakiris, G.; Pangalou, D.; Vangelis, H. Regional Drought Assessment Based on the Reconnaissance Drought Index (RDI). *Water Resour. Manag.* **2007**, *21*, 821–833. [CrossRef]
53. Shi, H.; Zhou, Z.; Liu, L.; Liu, S. A Global Perspective on Propagation from Meteorological Drought to Hydrological Drought during 1902–2014. *Atmos. Res.* **2022**, *280*, 106441. [CrossRef]
54. Shortridge, J.E.; Guikema, S.D.; Zaitchik, B.F. Machine Learning Methods for Empirical Streamflow Simulation: A Comparison of Model Accuracy, Interpretability, and Uncertainty in Seasonal Watersheds. *Hydrol. Earth Syst. Sci.* **2016**, *20*, 2611–2628. [CrossRef]
55. McCullagh, P.; Nelder, J.A. *Generalized Linear Models*; Springer: Boston, MA, USA, 1989; ISBN 978-0-412-31760-6.
56. Breiman, L. Random Forests. *Mach. Learn.* **2001**, *45*, 5–32. [CrossRef]
57. Aryal, J.; Sitaula, C.; Aryal, S. NDVI Threshold-Based Urban Green Space Mapping from Sentinel-2A at the Local Governmental Area (LGA) Level of Victoria, Australia. *Land* **2022**, *11*, 351. [CrossRef]
58. Li, L.; Xia, R.; Dou, M.; Ling, M.; Li, G.; Wang, C.; Mi, Q. Integrating Landsat NDVI Data with Climate and Anthropogenic Factors Reveals Drivers of Vegetation Dynamics in the Semi-Arid Basin of Western China. *Sci. Rep.* **2025**, *15*, 18831. [CrossRef] [PubMed]
59. Bhandari, A.K.; Kumar, A.; Singh, G.K. Feature Extraction Using Normalized Difference Vegetation Index (NDVI): A Case Study of Jabalpur City. *Procedia Technol.* **2012**, *6*, 612–621. [CrossRef]
60. Hashim, H.; Abd Latif, Z.; Adnan, N.A. Urban vegetation classification with ndvi threshold value method with very high resolution (vhr) pleiades imagery. *Int. Arch. Photogramm. Remote Sens. Spat. Inf. Sci.* **2019**, *XLII-4/W16*, 237–240. [CrossRef]
61. Idrees, M.O.; Omar, D.M.; Babalola, A.; Ahmadu, H.A.; Yusuf, A.; Lawal, F.O. Urban Land Use Land Cover Mapping in Tropical Savannah Using Landsat-8 Derived Normalized Difference Vegetation Index (NDVI) Threshold. *S. Afr. J. Geomat.* **2022**, *11*. [CrossRef]
62. Ainunnisa, I.; Haerani, H. The Identification of Pests and Diseases of Rice Plants Using Sentinel-2 Satellite Imagery Data at the End of the Vegetative Stage. *IOP Conf. Ser. Earth Environ. Sci.* **2023**, *1230*, 012148. [CrossRef]
63. Soriano-González, J.; Angelats, E.; Martínez-Eixarch, M.; Alcaraz, C. Monitoring Rice Crop and Yield Estimation with Sentinel-2 Data. *Field Crops Res.* **2022**, *281*, 108507. [CrossRef]
64. Katipoğlu, O.M.; Achite, M.; Kartal, V.; Çelik, M.A.; Pandey, K. Machine Learning-Based Hydrological Drought Prediction Integrating Teleconnections and Hydrological Memory in a Semi-Arid Basin, Algeria. *Atmosphere* **2026**, *17*, 670. [CrossRef]
65. Hou, J.; Van Dijk, A.I.J.M.; Beck, H.E.; Renzullo, L.J.; Wada, Y. Remotely Sensed Reservoir Water Storage Dynamics (1984–2015) and the Influence of Climate Variability and Management at a Global Scale. *Hydrol. Earth Syst. Sci.* **2022**, *26*, 3785–3803. [CrossRef]
66. Selek, B. Assessing Precipitation Memory and Operational Controls on National-Scale Reservoir Storage and Hydropower Dynamics in Türkiye. *Res. Sq.* **2026**. [CrossRef] [PubMed]
67. Kim, S.-J.; Bae, S.-J.; Lee, S.-J.; Jang, M.-W. Monthly Agricultural Reservoir Storage Forecasting Using Machine Learning. *Atmosphere* **2022**, *13*, 1887. [CrossRef]
68. Ahmed Osman, A.I.; AlDahoul, N.; Chong, K.L.; Huang, Y.F.; Ng, J.L.; Elshafie, A.; Sherif, M.; Ahmed, A.N. A Review on Machine Learning Models for Drought Monitoring and Forecasting. *Clim. Risk Manag.* **2025**, *50*, 100758. [CrossRef]
69. Özelkan, E. Spatial–Temporal Change of a Dam Lake Using Remote Sensing and Meteorological Drought Indices. In *Satellite Monitoring of Water Resources in the Middle East*; Shaban, A., Ed.; Springer Water; Springer International Publishing: Cham, Switzerland, 2022; pp. 129–147, ISBN 978-3-031-15548-2.

70. Coşkun, S. An Analysis of Water Scarcity in the City of Bursa Using Machine Learning in the Context of Climate Change and Population Scenarios. Master's Thesis, Bursa Uludağ University, Institute of Social Sciences, Department of Geography, Bursa, Türkiye, 2022.
71. Pham, H.; Vo, P.L. Impacts of Climate Change and Reservoir Operation on Droughts: A Case Study in the Upper Part of Dong Nai River Basin, Vietnam. *J. Water Clim. Change* **2025**, *16*, 511–530. [CrossRef]
72. Özelkan, E.; Chen, G.; Ustundag, B.B. Multiscale Object-Based Drought Monitoring and Comparison in Rainfed and Irrigated Agriculture from Landsat 8 OLI Imagery. *Int. J. Appl. Earth Obs. Geoinf.* **2016**, *44*, 159–170. [CrossRef]
73. Mohamadi, S.; Mianabadi, A.; Anvari, S. Investigating the Vegetation's Temporal–Spatial Response to Meteorological and Hydrogeological Drought in Drylands. *Geosci. Data J.* **2024**, *11*, 197–215. [CrossRef]
74. Nguyen, C.T.; Ton-That, L.; Pham, T.D. Land Use, Land Cover Changes and Expansion of Artificial Reservoirs in Eastern Thailand: Implications for Agriculture and Vegetation Drought Reduction. *Environ. Monit. Assess.* **2024**, *196*, 1009. [CrossRef] [PubMed]
75. Mliyeh, M.M.; Aqnouy, M.; Laaraj, M.; Bouizrou, I.; Tariq, A.; Benaabidate, L.; Kraiem, H.; Shitu, K. Assessing Drought Dynamics in a Semi-Arid Basin: A Multi-Index Approach Using Hydrological and Remote-Sensing Indicators. *Environ. Sci. Eur.* **2025**, *37*, 180. [CrossRef]
76. Schmitt, R.J.P.; Rosa, L.; Daily, G.C. Global Expansion of Sustainable Irrigation Limited by Water Storage. *Proc. Natl. Acad. Sci. USA* **2022**, *119*, e2214291119. [CrossRef] [PubMed]
77. Zhang, S.; Kang, Y.; Gao, X.; Chen, P.; Cheng, X.; Song, S.; Li, L. Optimal Reservoir Operation and Risk Analysis of Agriculture Water Supply Considering Encounter Uncertainty of Precipitation in Irrigation Area and Runoff from Upstream. *Agric. Water Manag.* **2023**, *277*, 108091. [CrossRef]
78. Shah, D.; Gao, H. Global Patterns of Reservoir Fullness and Fluctuations during Droughts. *Environ. Res. Lett.* **2025**, *20*, 124060. [CrossRef]
79. Warziniack, T.; Brown, T.C. The Importance of Municipal and Agricultural Demands in Future Water Shortages in the United States. *Environ. Res. Lett.* **2019**, *14*, 084036. [CrossRef]
80. Thomas, B.F.; Nanteza, J. Global Assessment of the Sensitivity of Water Storage to Hydroclimatic Variations. *Sci. Total Environ.* **2023**, *879*, 162958. [CrossRef] [PubMed]
81. Nakhaei, M.; Mohebbi Tafreshi, A.; Saadi, T. A Novel GIS-Based Modified Multivariate Drought Index for Modeling and Management of the Hydrogeological Drought (Case Study: Hashtgerd Aquifer, Iran). *Environ. Sci. Pollut. Res.* **2025**, *32*, 6005–6026. [CrossRef] [PubMed]

Disclaimer/Publisher's Note: The statements, opinions and data contained in all publications are solely those of the individual author(s) and contributor(s) and not of MDPI and/or the editor(s). MDPI and/or the editor(s) disclaim responsibility for any injury to people or property resulting from any ideas, methods, instructions or products referred to in the content.